Preliminary design of the FAIR Super-FRS superferric branched dipoles

ID Tue-Af-Po2.01-01

A. Madur, J. Muñoz-Garcia, L. Quettier, H. Allain, O. Rasamimanana, C. Pes, P. Graffin, H. Reymond (CEA)
H. Mueller, E. Cho, M. Winkler (FAIR/GSI)

Introduction :

CEA has the responsibility of the design studies for the superferric 1.6 T dipole magnets of the Superconducting FRagment Separator (Super FRS) which is part of the Facility for Antiproton and Ion Research (FAIR) in Darmstadt, Germany. After completing the study for the 21 superferric Super-FRS standard dipole magnets, CEA is currently analysing conceptual solutions for the 3 superferric branched dipole magnets. Branched dipole magnets are necessary to allow the separated particles to be directed along each of the three branches of the separator. The branched dipoles will keep most of the features incorporated in the standard dipole magnet design but they will have increased complexity to make them compatible with the vacuum chamber layout at the branches locations (Y-shape). The magnetic design of the yoke will be slightly modified whereas a new cryogenic design is required. We present here the design concepts envisioned for the FAIR Super-FRS branched dipole magnets along with preliminary design simulation results (magnetic, cryogenic and mechanical analyses).

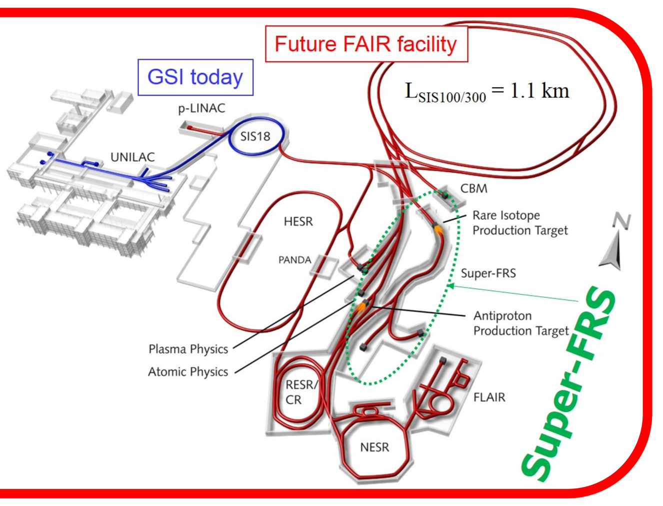

Design & parameters

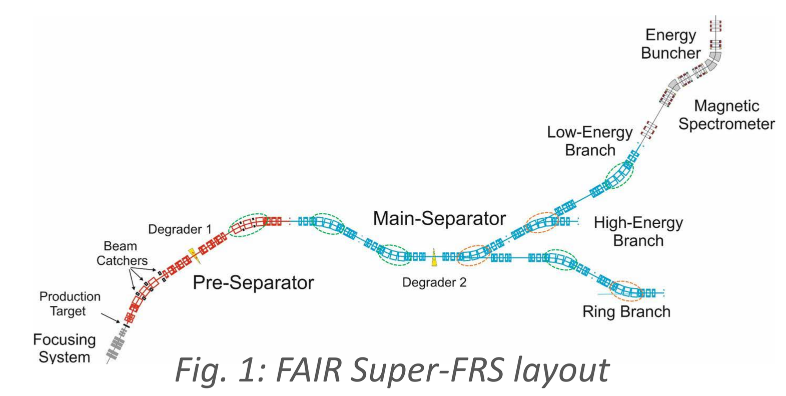

Fig. 1: FAIR Super-FRS layout

Maximum beam rigidity	20 T.m
Bending angle	9.75 °
Bending radius	12.5 m
Maximum dipole flux density	1.6 T
Maximum integrated dipole flux density	3.4 T.m
Integrated flux density homogeneity	+/- 3. 10^{-4}
Pole gap height	170 mm
Elliptical good field region height	140 mm
Elliptical good field region width	380 mm

Table 1: Specifications for the Super-FRS branched dipoles

The yoke geometry is straight in the longitudinal direction (not curved), it has an H cross-section and is trapezoidal when viewed from the top. The NbTi coils also have a trapezoidal shape and keep the standard cross-section with 560 turns.

Conductor width (bare)	1.97 mm
Conductor thickness (bare)	1.17 mm
Insulation thickness	0.13 mm
Core wire bare diameter	0.715 mm
Filament diameter	0.065 mm
Cu/SC ratio	11
RRR	>80
Electrical current at 4T, 4.22 T (guaranteed)	660 A
Current margin at 1.6 T	74%

Table 2: NbTi conductor parameters

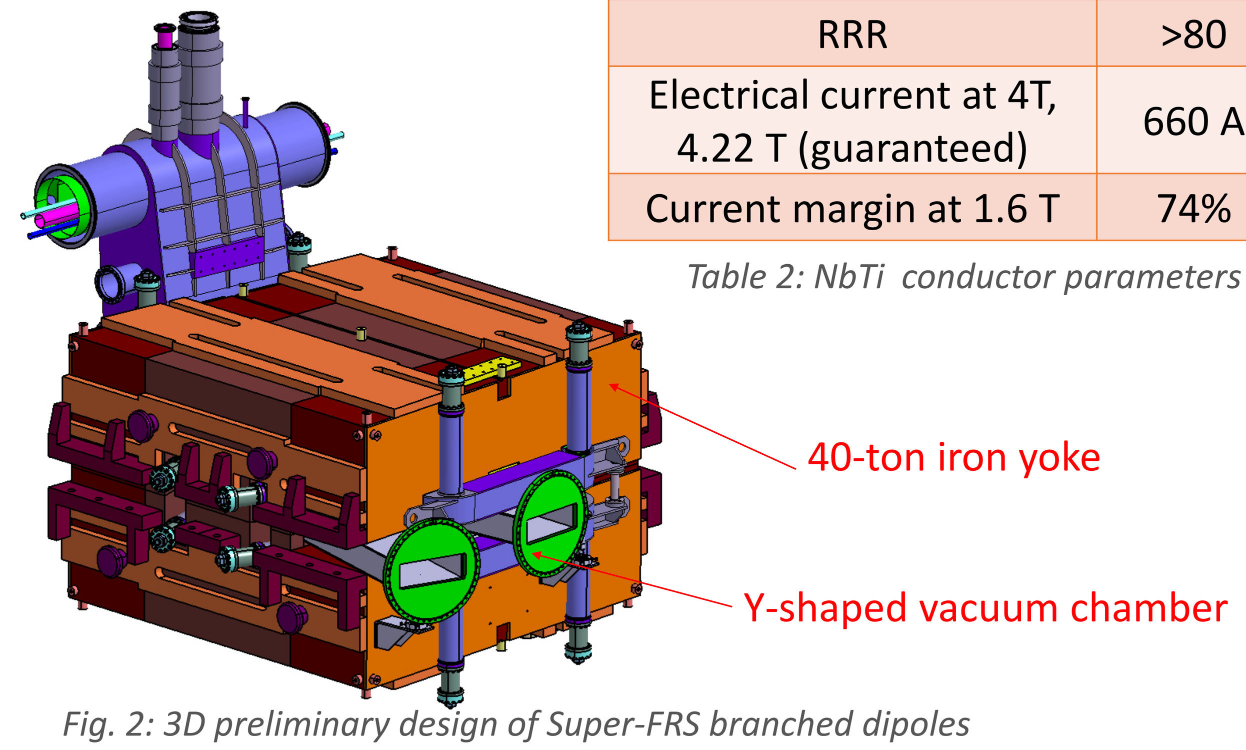

Fig. 2: 3D preliminary design of Super-FRS branched dipoles

Magnetics

- Clearance for Y-shaped vacuum chamber
- Larger opening for cold to warm supports
=18 % of the standard dipole yoke volume has been removed

B_0	0,15 T		1,0 T		1,6 T	
Magnet type	Std	Br.	Std	Br.	Std	Br.
Bpeak [T]	0.12	0.12	0.79	0.868	1.44	1.86
I [A]	18.25	18.25	123.2	128.6	246.5	293.9
E [kJ]	3.8	3.8	171.5	183.1	455.7	507.4

Table 3: Magnetic simulation results comparison

More amp-turns are needed for the branched magnet version to reach the same field at the center.

As a consequence, this increases the peak field on the conductor and the stored energy but they remain manageable from the protection point of view.

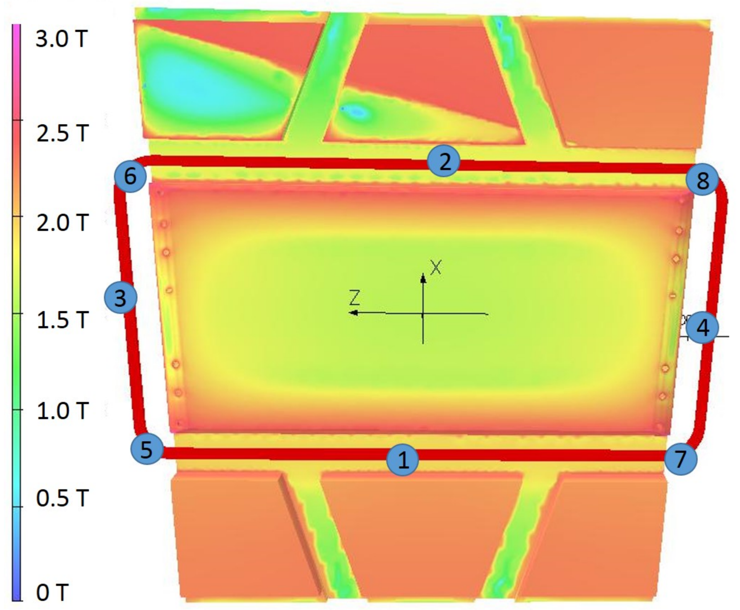

Fig. 3: Flux density distribution in yoke

The chamfers have been optimized to get the required homogeneity: the alignment slot and the holes for the screws have been slightly moved to the sides (see Fig. 3)
These chamfer holes asymmetries can Looking at the homogeneity map, one can locate the chamfers holes through the blue to red areas at z = +/-70 mm.
Two spots in the midplane located at y = +/- 190 mm which shows the homogeneity perturbations due to the openings in the yoke sides

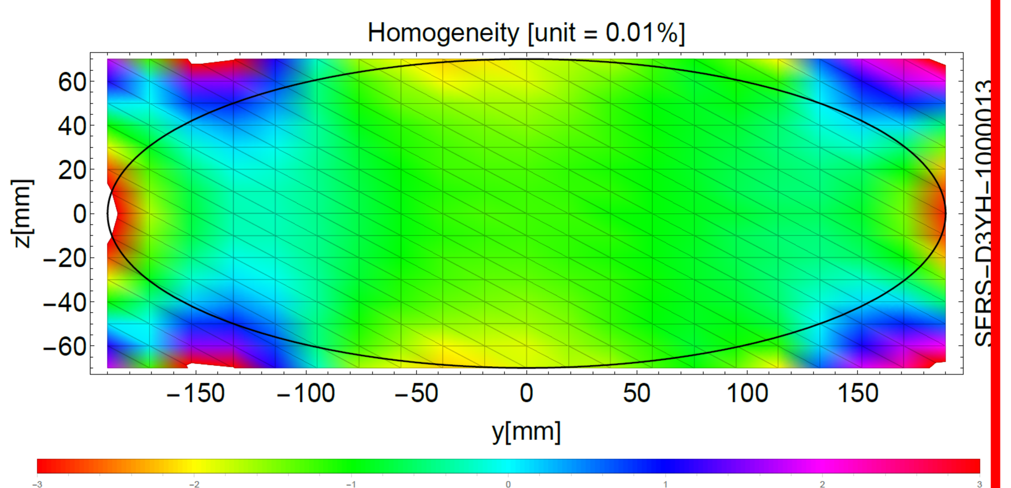

Fig. 4: Flux density integral homogeneity

Mechanics

The standard cryostat has been split in the mid plane leading to two independent cryostats (top with the cryo-tower and bottom) which are connected at one of the entrance corners for vacuum, cryogenics, electrical and instrumentation utilities.
A bellow is connecting the top and bottom cryostat to align them independently. The cryostats are directly mounted to the yoke through the grey ears. Then one end of each cold-to-warm-support (CTWS) is mounted on the vacuum vessel while the other is connected to the floating coil casing for alignment and support purpose.

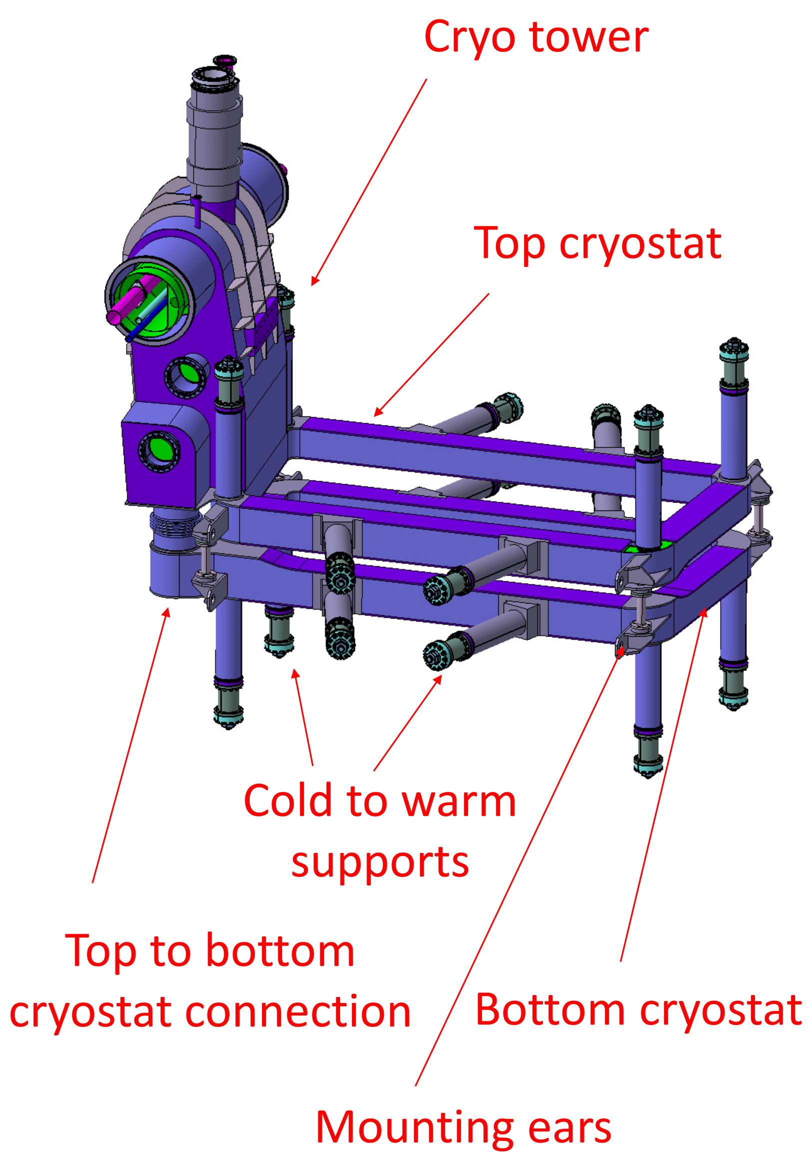

Fig. 5: Details of the cryostat design

	Standard [kN]			Branched [kN]		
cond. #	Fx	Fy	Fz	Fx	Fy	Fz
1	-46.9	93.3	0	-29.4	104.7	0
2	50.9	98.8	0	48.3	143	0
3	-1.9	20.8	22.6	-2	20.7	23.6
4	-1.9	20.8	-22.6	-2	20.7	-23.6
5	-4.7	4.3	4.3	-5.3	4.4	5.1
6	4.9	4.3	5.3	5.9	6.1	6.3
7	-4.7	4.3	-4.3	-5.4	4.4	-5.1
8	4.9	4.7	-5.3	5.4	5.1	-6.1

Table 4: Lorentz forces comparrison

The observed Lorentz force asymmetries are mainly due to the asymmetric magnetization of the yoke introduced by the additional clearance needed for the Y-shaped vacuum chamber. The independent coil casings will be too weak to contain the outward vertical forces. Cold-to-warm contacts (CTWC) in the straight element region between the coil groove of the yoke and the coil are under investigation.

Cryogenics

The coil is cooled by a 20 x 10 mm² liquid helium channel (4.4 K, 1.2 bar). The 50 K thermal shield is cooled through brazed pipes with circulating 50 K helium gaz. There will be 30 layers of Multi-layer insulation.

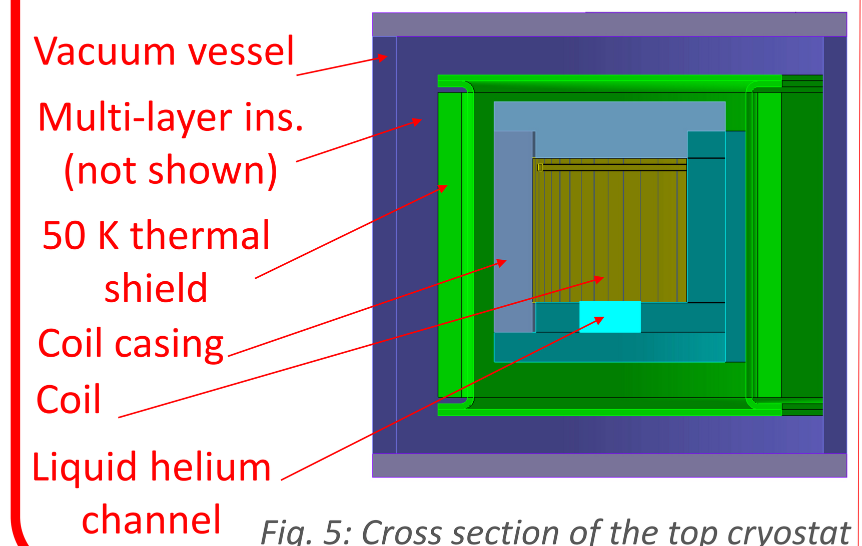

Fig. 5: Cross section of the top cryostat

Active thermosiphon concept

Each coil will have an independent helium circuit. In a passive thermosiphon, the heat exchange is done on the vertical exit tube so that the helium weight unbalance between the entrance and exit generates a mass flow to cool the coil.

For design constraint reasons the heat exchange is horizontal (coil vs helium channel) therefore heaters will be installed on the exit tube to actively initiate the needed mass flow.

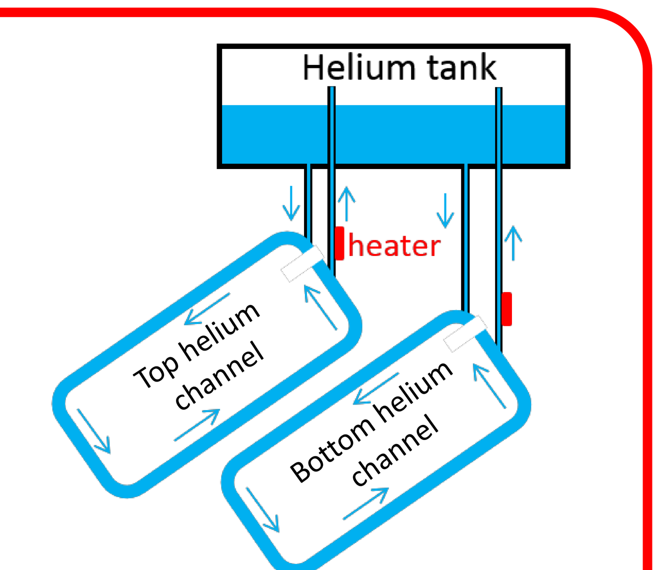

Fig. 5: Principle of active thermosiphon

	Cold mass	Thermal-shield
Radiation	2.7 W [0.3 W/m²]	27 W [3 W/m²]
Conduction	3.2 W (0.2 W/sup.)	128 W (8 W/sup.)
Current leads	0.04 g/s	
Total	5.9 W + 0.04 g/s	145 W

Table 5: Preliminary heat load budget

Next steps

If the design is rather well defined from the magnetic point of view, there are still several analyses to carry out on the mechanical (cold to warm contacts) and cryogenics (active thermosiphon stability) aspects. CEA plans on proposing a final design to FAIR/GSI during the Summer of 2018